Phosphor-Converted Laser-Based Illuminant With High Color Rendering Index and Low Blue Light Hazard

Lei Ye, Xinglin Peng, Jie Yang, Xuejian Liu, Zehua Liu, Hua Yang, Ping Chen, Zhe Liu, and Yun Zhang

***Abstract*—Laser-based illuminant has been a topic of increasing interest in recent years and both of color quality and blue light hazards are the key issues that need to be addressed. In this paper, the performances of color quality and blue light hazard were investigated by comparing 465 nm laser-excited phosphor materials and traditional 452 nm laser-excited phosphor materials respectively. Phosphor-converted laser-based illuminant (pc-LBI) consisting of 465-nm and 635-nm LDs (LBI-465) has a color rendering index (CRI) of 88.7, which was 8.2% higher than that of pc-LBI consisting of 452-nm and 635-nm LDs (LBI-452). The correlated color temperature (CCT) of white light of both pc-LBIs ranges from 2200 K to 5000 K with the adjustment of red lasers. The blue light hazard efficiency of radiation (BLHER) of LBI-465 is below 0.15, which is 19% lower than that of LBI-452. The results showed that high color quality and low blue light hazard were simultaneously achieved by LBI-465. In addition, the above experimental results are in good agreement with the simulated results. Based on these above results, pc-LBI is believed to render laser-based white light sources with good color performance and boost the growth of solid-state lighting.**

Manuscript received 5 July 2022; accepted 7 July 2022. Date of publication 12 July 2022; date of current version 20 July 2022. This work was supported in part by the National Natural Science Foundation of China under Grant 61674143 and in part by the Science and Technology Project of Technology Commission Foundation of Beijing under Grant Z211100004421013. *(Corresponding author: Zhe Liu.)*

Lei Ye, Jie Yang, Zhe Liu, and Yun Zhang are with the Laboratory of Solid State Optoelectronics Information Technology, Institute of Semiconductors, Chinese Academy of Sciences, Beijing 100083, China, and also with the Center of Materials Science and Optoelectronics Engineering, University of Chinese Academy of Sciences, Beijing 100049, China (e-mail: yelei25@semi.ac.cn; jieyang@semi.ac.cn; liuzhe@semi.ac.cn; yzhang34@semi.ac.cn).

Xinglin Peng and Xuejian Liu are with the State Key Laboratory of High-Performance Ceramics and Superfine Microstructure, Shanghai Institute of Ceramics, Shanghai 200050, China, and also with the Center of Materials Science and Optoelectronics Engineering, University of Chinese Academy of Sciences, Beijing 100049, China (e-mail: pengxinglin@student.sic.ac.cn; xjliu@mail.sic.ac.cn).

Zehua Liu is with the Ningbo Institute of Materials Technology and Engineering, Chinese Academy of Sciences, Ningbo 315201, China, and also with the Center of Materials Science and Optoelectronics Engineering, University of Chinese Academy of Sciences, Beijing 100049, China (e-mail: liuzehua@nimte.ac.cn).

Hua Yang is with the State Key Laboratory of Solid-State Lighting, Institute of Semiconductors, Chinese Academy of Sciences, Beijing 100083, China, and also with the Center of Materials Science and Optoelectronics Engineering, University of Chinese Academy of Sciences, Beijing 100049, China (e-mail: huayang@semi.ac.cn).

Ping Chen is with the State Key Laboratory of Integrated Optoelectronics, Institute of Semiconductors, Chinese Academy of Sciences, Beijing 100083, China, and also with the Center of Materials Science and Optoelectronics Engineering, University of Chinese Academy of Sciences, Beijing 100049, China (e-mail: pchen@semi.ac.cn).

Digital Object Identifier 10.1109/JPHOT.2022.3190000

***Index Terms*—Laser-based illuminant, color quality, blue light hazard.**

I. Introduction

SOLID-state lighting (SSL) has been widely applied as a white light source because of its longevity, high efficiency and environmental friendliness [1], [2]. Phosphor-converted light emitting diodes (pc-LEDs) are the mainstream commercial white light sources [3]. The highest efficiency of LEDs tends to appear at a current density of $\sim$0.01 kA/cm^2 due to the inevitable "efficiency droop". In contrast with LEDs, laser diodes (LDs) can maintain high efficiency at high current densities $>$10 kA/cm^2 because of stimulated radiation [4]–[6]. LD-driven white lighting has great potential in high luminance lighting, such as projector technology, automobile headlights and medical endoscopy [7]–[9]. LDs also exhibit these unique characteristics, including directional beam patterns and compact sizes [10]. The light beam of LDs is more easily coupled into plastic optical fibers than that of LEDs, which separates the lighting parts from electricity and allows LD-based white light sources to be applied in hazardous environments [11]. Therefore, LD-based white illuminants will play an important role in special lighting with multifunctional scenes.

The laser-based lighting systems usually consist of blue LDs and phosphor converter, where the color quality of pc-LBI is significant for practical applications based on LDs [12], [13]. The most commonly used method of phosphor-converted LD-based illuminant (pc-LBI) is fabricated by 440–455 nm blue LDs and yellow phosphor materials [14]. The color rendering index (CRI) of pc-LBI is always below 70 and its correlated color temperature (CCT) is above 6000 K due to lack of red emission components, which is undesirable for laser lighting through the yellow phosphors under the excitation of blue LDs [15]–[17]. Many researchers have paid their attention to red phosphors [18], [19]. The $Mg_2Al_4Si_5O_{18}$:Eu^{2+} composite phosphor driven by 450-nm blue LD exhibited a CRI of 85.2 and a CCT of 4146 K [20]. High CRI of 88 and a CCT of 8665 K were achieved through $CaAlSiN_3$:Eu^{2+}/$Lu_3Al_5O_{12}$:Ce^{3+} driven by 455-nm blue LDs [21]. However, strict preparation requirements and microstructure make red phosphors difficult to fabricate [22], [23]. Red phosphors cannot tolerate the high-power output of blue LDs. Red LDs are also used to improve the CRI of pc-LBI and suitable for high power output [24], [25]. The addition of red LDs renders

the fabricated freedom of pc-LBI and efficiently improve the color quality of pc-LBI. In addition to the important role of red light spectrum on color quality, blue LDs and its coupling mechanism with phosphor materials are also crucial. The 440–455 nm blue LDs are adopted in most of reports for now and there are few researches on other blue wavelength. The interaction mechanism of phosphor materials and red/blue LDs should be considered.

Another concern of pc-LBI is blue light hazard (BLH). Some solutions have been studied [26], [27], such as decreasing the blue power ratio of the spectral power distribution in a white light system [28], [29]. Moreover, some studies have shown that the short wavelength ranging from 415 nm to 460 nm has more serious BLH than other blue wavelengths [30], [31]. So, the choice of blue wavelength also needs to be considered. In addition, the residual proportion of blue light also affects the co-optimization of CRI and BLH of white light system. Many studies on BLH and color performance have been conducted on multicolor LEDs [32], [33]. Studies on laser lighting concerning BLH are rarely reported. It is proposed that the spectral power distribution of the potential laser lighting should be optimized for low BLH. Apart from low BLH and high color quality, the circadian effect is also elicited by the blue light, which can entrain the circadian system [34]–[36].

In this work, the performance of color quality and blue light hazard were investigated by comparing 465 nm laser-excited phosphor materials (LBI-465) and traditional 452 nm laser-excited phosphor materials (LBI-452) respectively. The optical power ratio of blue LD to red LDs for pc-LBI was taken into consideration to improve the CRI and CCT. The CRI of the LBI-465 is 88.7, which is 8.2% higher than that of the LBI-452. The BLH values of LBI-465 are below 0.15. Both approaches with two blue wavelengths can meet the different demands of white lighting situations with CCT ranging from 2200 K to 5000 K by tuning the power ratio of red to blue LDs. The experimental results agree well with the simulated values. It is evaluated that the highest CRI value can be further improved to 90 by appropriate proportion of 465 nm LDs to red LDs.

II. Schematic and Theory

A. Experimental Setup

Schematic illustration of the pc-LBI system consists of LD modules, optical fibers, and a phosphor converter in Fig. 1(a). The traditional LBI-452 consisting of 452-nm LDs and 635-nm LDs and LBI-465 consisting of 465-nm LDs and 635-nm LDs were made for comparison. The 635 nm LD with full width at half maximum (FWHM) of 3 nm emits a maximum output power of 1 W with the threshold current of 0.40 A. The 452-nm LD with FWHM of 4 nm emits a maximum output power of 4 W with the threshold current of 0.5 A. The 465-nm LD with FWHM of 4 nm emits a maximum output power of 2.5 W with the threshold current of 0.4 A. All LD modules are encapsulated in the copper inner case for better heat dissipation. The optical fibers with a core diameter of 105 μm and a numerical aperture (NA) of 0.22 connect the LD modules and are coupled into a 400 μm core optical fiber with a NA of 0.22. The light from the phosphor converter is collected by a 2-metre Labsphere integrating sphere.

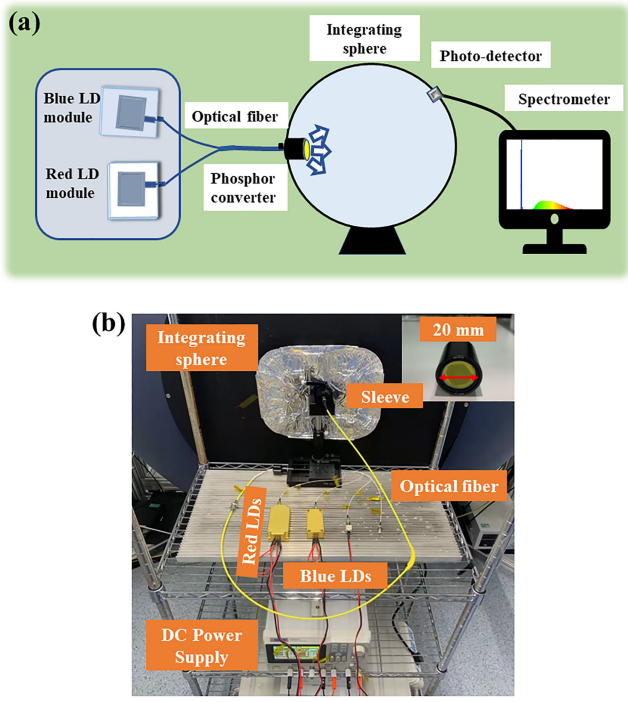

Fig. 1. (a) Schematic illustration of the construction. The inset shows the emission spectra of an Al_2O_3-YAG:Ce^{3+} phosphor plate driven by the 452-LD module. (b) Photograph of the measurement setup of pc-LBI.

Then, the spectral power distribution and color parameters of pc-LBIs are shown on a computer screen. The photograph of the measurement setup shows LD modules with a DC power supply and the integrating sphere in Fig. 1(b). The inset shows the sleeve containing an Al_2O_3-YAG:Ce^{3+} phosphor plate. The Al_2O_3-YAG:Ce^{3+} phosphor plate is 20 mm in diameter and 0.2 mm in thickness. The optical fiber has four fiber lines for three-wavelength LD modules. This module design has the benefit of individually tuning each LD to control the output power.

B. Phosphor Preparation

YAG:Ce^{3+} phosphors (Intematix Co., USA) and α-Al_2O_3 (Taimei Chemicals Co., Japan) were used as raw materials. With a weight ratio of YAG:Ce^{3+}: Al_2O_3 = 1:4, the powder mixture was ball- milled with a powder to Al_2O_3 ball ratio of 1:2 for 12 hours at a rotation speed of 150 r/min. Then the mixed powder was passed through a 200-mesh sieve. The mixed powder was densified by Spark Plasma Sintering (SPS) technique. The graphite mold interior was lined with carbon paper and 2.5 g of powder was added. The outside of the graphite mold was covered with a thermal insulator carbon felt. A heating rate of 100°C/min and a uniaxial pressure of 80 MPa were applied. The samples were sintered at 1452°C and the holding time was 20 min. The sintered samples were kept in a muffle furnace at 1200°C for 10 hours in an air atmosphere to remove the carbon contamination caused by SPS, and it also played a role in eliminating thermal stress. The sintered samples were carefully machined and then double-side polished to 0.2 mm for subsequent characterizations.

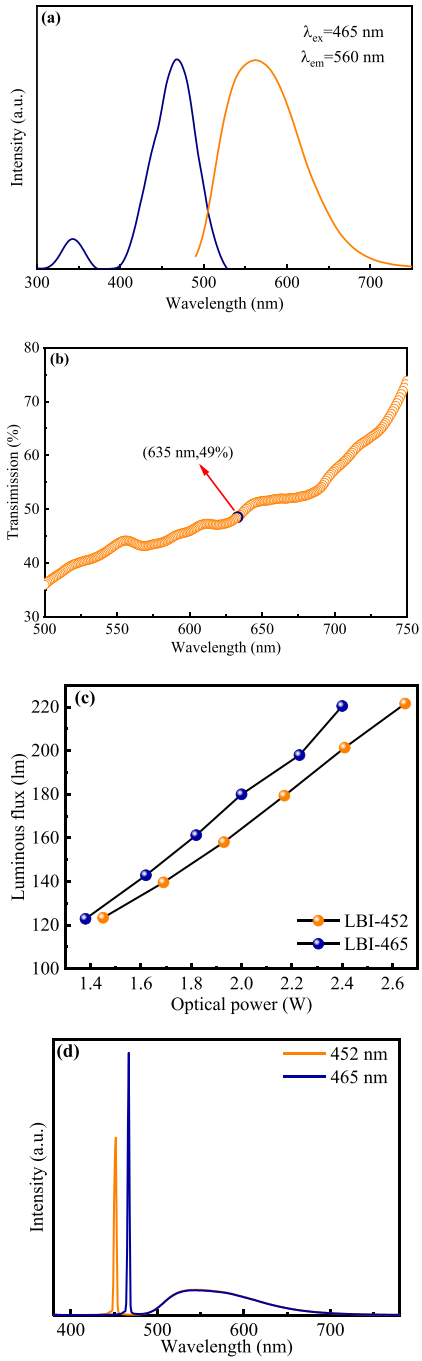

Fig. 2. (a) The excitation and emission spectra of Al_2O_3-YAG:Ce^{3+}. (b) Transmittance spectrum of Al_2O_3-YAG:Ce^{3+}. (c) Luminous flux of Al_2O_3-YAG:Ce^{3+} driven by different optical powers of 452-nm and 465-nm LD modules. (d) Luminescence spectra of Al_2O_3-YAG:Ce^{3+} under the excitation of 2.65 W 452 nm LD and 2.4 W 465 nm LD, respectively.

The photoelectric properties of the phosphor converter Al_2O_3-YAG:Ce^{3+} are displayed in Fig. 2. The excitation and emission spectra of Al_2O_3-YAG:Ce^{3+} were recorded on a steady-state fluorescence spectrometer (FLS920, Edinburgh Instruments, U.K.) in Fig. 2(a). The spectra exhibited strong yellow light emission at 560 nm under 465-nm wavelength irradiation. The transmittance spectrum was measured by a UV-VIS-NIR spectrophotometer (Lambda 950, PerkinElmer, USA), as shown in Fig. 2(b). The transmittance of Al_2O_3-YAG:Ce^{3+} at 610 nm, 615 nm, 620 nm, 625 nm, 630 nm, 635 nm and 640 nm is 47.2%, 47.2%, 47.1%, 47.3, 48.0% and 49%.

Based on the measurement setup, the Al_2O_3-YAG:Ce^{3+} phosphor converter was driven by 452-nm LD and 465-nm LD. By controlling the power of the two blue LD modules, the luminous flux values of the two pc-LBIs were the same. In the experiment, the luminous flux is kept 220 lm, which corresponds to 2.4 W 465 nm LD and 2.65 W 452 nm LD, respectively. The experimental results of luminous flux of LBI-452 and LBI-465 under different optical powers are shown in Fig. 2(c). The luminescence spectra of Al_2O_3-YAG:Ce^{3+} under the 2.65 W 452 nm LD and that under the 2.4 W 465 nm LD excitation are shown in Fig. 2(d). It can be calculated that the conversion efficiency of the phosphor under the excitation of 452 nm LD is 21.5% while that under the excitation of 465 nm LD is 23.2%. It means that the efficiency of Al_2O_3-YAG:Ce^{3+} phosphor converter under 465 nm LD excitation is higher than that under 452 nm LD excitation. Apart from phosphor's conversion efficiency, the wall plug efficiency is 38% for 452 nm LD and 26.5% for 465 nm LD, respectively. The optical fiber coupling efficiency is up to 85% for the LD module. Therefore, the total efficiency is 5.2% for 465 nm LD module which is slightly lower than that for the 452 nm LD module (6.9%). It will be addressed by the improvement of the wall plug efficiency of 465 nm LD in future work. The optical power ratio of yellow light to the remained blue light for LBI-452 is 4.7 while that for LBI-465 is 4.2. It shows that the remained blue light of LBI-465 is more than that of LBI-452, which leads to the higher CCT of LBI-465 compared with that of LBI-452 in Section III.

C. Calculation Model

1) Method to Improve CRI: To improve the CRI of pc-LBI, the spectral power distribution of emission spectrum from pc-LBI and red LDs is considered. We assumed that the peak wavelength and FWHM of blue LDs and red LDs are constant [37], [38]. So, the spectral power distribution of emissive pc-LBI will be linearly combined with the spectral power distribution of red emissive parts.

The spectral power distribution of pc-LBI and red LDs is given by [39],

$$S\ (\lambda) = H_{pc}\ P_{pc}\ (\lambda) + H_r P_r\ (\lambda, \lambda_n, w_n) \tag{1}$$

where H_{pc} is the relative power of pc-LBI and H_r is the power of red LD. $P_{pc}(\lambda)$ is the relative spectral power distribution of Al_2O_3-YAG:Ce^{3+} phosphor plate driven by blue LD, which can be measured by the integrating sphere. $P_r(\lambda, \lambda_n, w_n)$ refers to the relative spectral power distribution of red LDs at different wavelength (λ). Here, the transmittance of Al_2O_3-YAG:Ce^{3+} should be considered. λ_n and w_n refer to peak wavelength and FWHM of different emissive parts. Considering the small FWHM and symmetrical spectral power distribution of LD, Gaussian formula is used to describe the relative spectral distribution, which is given by,

$$P(\lambda, \lambda_n, w_n) = e^{-k\left(\frac{\lambda-\lambda_n}{w_n}\right)^2} \tag{2}$$

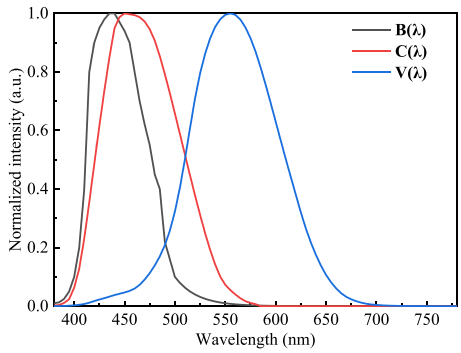

Fig. 3. Blue light hazard spectral weighting function B(λ), circadian spectral sensitivity C(λ) and photopic vision function V(λ) referring to wavelengths from 380 nm to 780 nm.

where k is constant. Although multiple-emission spectra play a positive influence on the improvement of CRI, it inevitably leads to the complexity of fabrication and the rising cost. The emissive parts here are controlled to two parts, which simplify the calculation process. To calculate the CRI, the comparison of color appearance from 14 CRI reflective samples is done when they are illuminated by a reference illuminant and the light source pc-LBI under test. Referring to the literature [40], general CRI (Ra) of the tested pc-LBI is calculated. If Ra is 100, it means that there is no color difference between tested light sources and the reference illuminants.

2) Method to Calculate BLH and CAF: The BLH is estimated by the blue light hazard spectral weighting function (B(λ)). Circadian spectral sensitivity (C(λ)) refers to the nonvisual spectral response curve or the circadian weighting function, which is related with the circadian effect. Photopic vision function (V(λ)) shows the human eye's visual response to different wavelengths, which is relevant to the luminous flux and luminous efficiency of the light source. The above three-function curves for wavelengths of 380–780 nm are shown in Fig. 3.

Therefore, the blue light hazard efficiency of radiation (BLHER) is defined as the ratio of blue light hazard quantity to the corresponding radiometric quantity, which can be expressed as [41]:

$$BLHER = \frac{\sum_{380}^{780} S(\lambda) B(\lambda) \Delta\lambda}{\sum_{380}^{780} S(\lambda) \Delta\lambda} \tag{3}$$

where S(λ) is the spectral power distribution of the light source, B(λ) is the blue hazard spectral weighting function, and Δλ is the wavelength interval (1 nm in this work). The circadian rhythm factor (CAF) is defined as the ratio of the circadian efficiency to luminous efficiency and is obtained as follows [34]:

$$CAF = \frac{K \sum_{380}^{780} S(\lambda) C(\lambda) \Delta\lambda}{\sum_{380}^{780} S(\lambda) V(\lambda) \Delta\lambda} \tag{4}$$

where K is the normalization constant, which makes CAF = 1 for the CIE standard illumination D65. C(λ) peaks at approximately 464 nm, while V(λ) peaks at 555 nm.

III. Results and Discussions

A. Color Performance of PC-LBI With Red LDs

The experimental and simulated results of CRI and CCT for 220-lm LBI-452 and 220-lm LBI-465 under different power ratios of red LDs and blue LDs are shown in Fig. 4(a) and 4(b), where the power ratio of red and blue LDs ranged from 0 to 0.5. The CRI of LBI-465 and LBI-452 had the similar variation tendency and both reached their peak values at the power ratio of 0.2. When the power ratio was above 0.2, the CRI of both pc-LBIs dropped and the CRI of LBI-465 was slightly lower than that of LBI-452. It has been proved that the power ratio of red light and blue light has a great influence on the CRI of pc-LBIs. The CRI of LBI-452 was improved by 30.7% from 62.6 to 81.8 and the CRI of LBI-465 was improved by 36.9% from 64.8 to 88.7. It should be noticed that the CRI of LBI-465 reached 88.7, which was 8.2% higher than that of LBI-452 under the power ratio of 0.2. The simulated CRI values agree well with the experimental CRI, for example the highest simulated CRI is 88.3, which was 0.45% deviation from the experimental CRI in Fig. 4(a). The CRI value is satisfactory and higher than those in the recent reports about LBIs [14], [16], [20]–[22], [42] and it is also comparable with those of pc-LEDs benefiting from the broadband emission [20], [43], [44]. As shown in Fig. 4(b), the simulated CCT of LBI-452 was slightly lower than that of LBI-465 because there is more blue light component in LBI-465 than LBI-452 in Fig. 2(d). Moreover, the increasing red component in pc-LBIs leaded to decreasing CCT, which means that the different power ratio of red LDs and blue LDs can be applied to different requirements of white lighting situations. The simulated results shows that the designed power ratio of bichromatic LBI is of great importance. Compared with the simulated and experimental data of CRI and CCT, the same variation trend was observed. The deviation of CCT between the simulated results and experimental results was below 100 K. The high CRI and low CCT are achieved simultaneously through spectral optimization method compared with the literature [14], [16], [22].

The CIE coordinates of LBI-452 and LBI-465 are shown in Fig 4(c). The CIE coordinates of LBI-452 and LBI-465 under the optical power ratio of red/blue LDs from 0 to 0.5 are shown in Fig 4(c). As the optical power of red LD, the CIE x of both LBIs increases while the CIE y of both LBIs decreases. Under the power ratio of 0.2, the CIE color coordinates of LBI-465 and LBI-452 are (0.4007, 0.3998) and (0.4088, 0.3862), respectively. Duv means the distance from light sources to the Planckian locus on the chromaticity coordinates. The Duv values for LBI-452 and LBI-465 were calculated to be −0.0027 and 0.0050, respectively. The Duv of both pc-LBIs meets the constraints, less than 0.0054 [45]. The color fidelity score (Rf) and color gamut score (Rg) have been proposed to evaluate the color fidelity of white light sources more sensitively and accurately [46], [47]. The calculated Rf and Rg of LBI-452 and LBI-465 under the optical power ratio of red LDs and blue LDs from 0 to 0.5 are shown in Fig 4(d). The Rf of both LBI-452 and LBI-465 is more than 80 and Rg is more than 90 when the optical power ratio of red/blue LDs is 0.2. So, the spectral power distribution

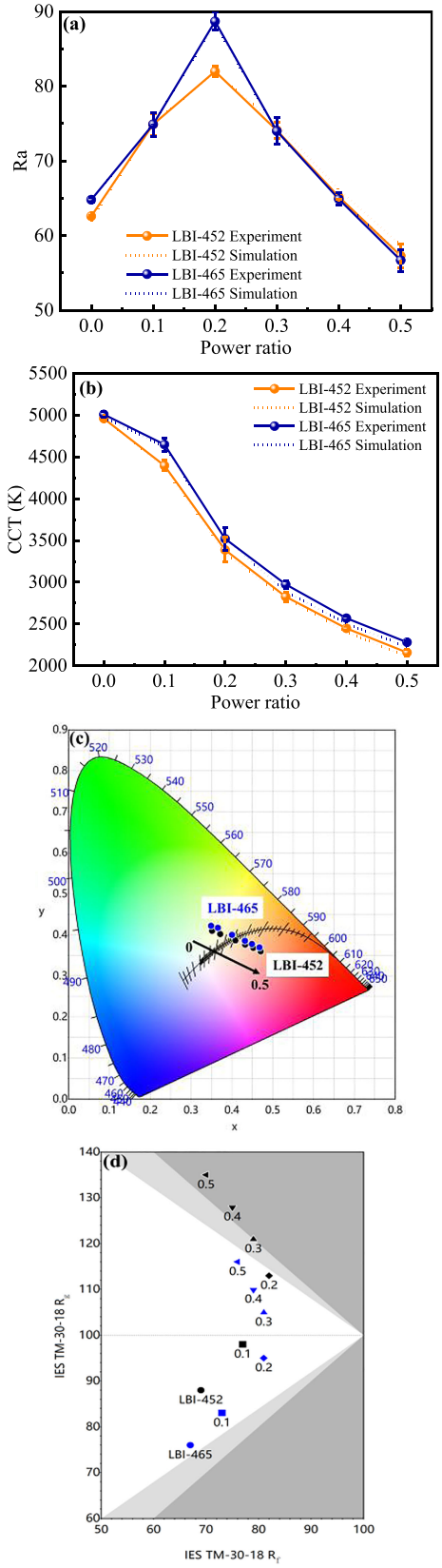

Fig. 4. Experimental and simulated results of (a) CRI and (b) CCT for LBI-452 and LBI-465 with a luminous flux of 220 lm under the optical power ratio of red LDs and blue LDs from 0 to 0.5. (c) CIE coordinates and (d) calculated Rf and Rg of LBI-452 and LBI-465 under the optical power ratio of red LDs and blue LDs from 0 to 0.5.

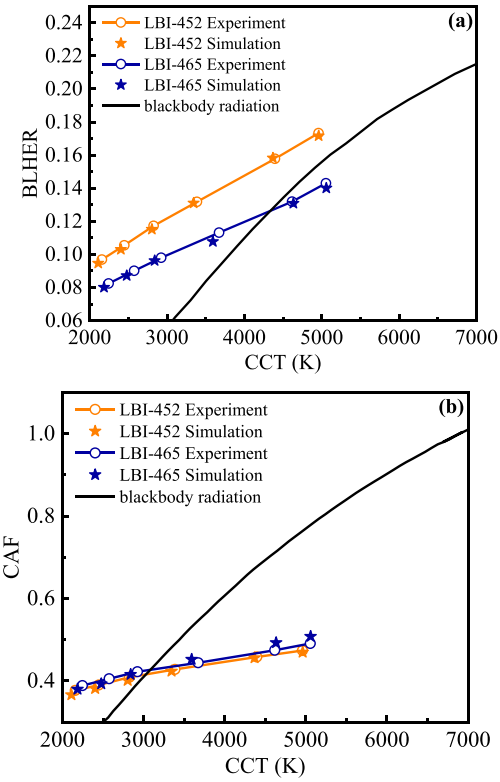

Fig. 5. The (a) BLHER and (b) CAF of the pc-LBIs at different CCTs, where the blackbody radiation is shown for comparison.

optimization method is a feasible way to fabricate good-quality white light illumination.

B. BLH and CAF of pc-LBI With Red LDs

Health issues regarding blue light hazard and circadian effects are important. Therefore, there is an urgent need to consider healthy lighting while achieving high color performance. The BLHER is calculated under different power ratios and compared with blackbody radiation, as shown in Fig. 5(a). The BLHERs of LBI-465 and LBI-452 were below 0.15 and 0.18, respectively. The BLHER decreased with the increase of red LD power. Under the optical power ratio of red/blue LDs of 0.2, the BLHER of LBI-465 is 0.113, which is comparable with good results of the literatures [33], [36], [47]. The BLHER of LBI-452 is on average 19% higher than that of LBI-465. It can be understood that 452 nm is the peak wavelength in B(λ) while 465 nm is far away from the peak wavelength (415 nm-460 nm), as shown in Fig. 3. When the power ratio increases from 0 to 0.5, BLHER decreases accordingly because the blue component ratio of both pc-LBIs also decreases [25]. The experimental results agree well with the simulated values. Although the BLHER of both pc-LBIs is higher than that of blackbody radiation, it is demonstrated that longer blue wavelengths can efficiently reduce BLH.

The variation in experimental and simulated CAF with increasing CCT is shown in Fig. 5(b). The varying trend of CAF with different CCT is similar for both pc-LBIs, where the CAF is ascending with the increasing CCT. The CAF of both pc-LBIs ranges from 0.35 to 0.50. However, the CAF of LBI-465 is

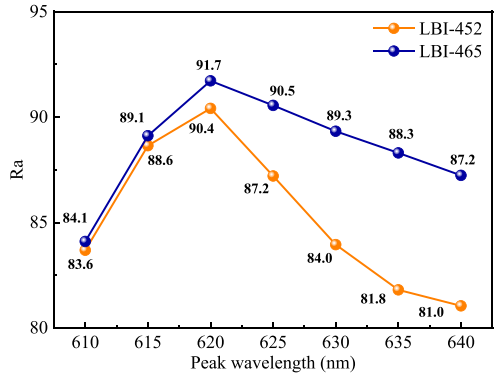

Fig. 6. The simulated Ra of LBI-452 and LBI-465 with different red wavelengths under an optical power ratio of 0.2.

higher than that of LBI-452 at CCTs from 2200 K to 5000 K. A higher CAF is caused by a greater proportion of blue light in the pc-LBI. Although the pc-LBIs were comprised of blue and red LDs, the CAFs of both pc-LBIs were lower than that of blackbody radiation when CCTs were higher than 3000 K. Studies have shown that mixed white light with low CCT and low CAF is helpful for sleep quality [26]. It can be concluded that LBI-465 with low BLHER and low CAF has potential for bedroom lighting. Further study should focus on how to decrease BLH and tune the CAF, such as multicolor LDs system.

C. Prediction of CRI

The wavelength of red LDs was considered in order to investigate the trend of CRI and BLH. The peak wavelength of red LDs ranging from 610 nm to 640 nm with the interval of 5 nm was combined with LBI-452 and LBI-465 under the power ratio of red LDs to blue LDs is 0.2. It is assumed that the FWHM of red LDs is 3 nm. From the above simulation and experimental results, it can be concluded that the CRI value of pc-LBI reach the highest under the power ratio of 0.2. The simulated CRI of LBI-452 and LBI-465 increased from 610 nm to 620 nm, and reached the peak at 620 nm in Fig. 6. Then, the CRI of LBI-465 decreased more slowly than that of LBI-452 as the red wavelength increased from 620 nm to 640 nm. Moreover, the CRI of LBI-465 were above that of LBI-452 at the same wavelength. It is concluded that LBI-465 combined with short red wavelength can achieve higher CRI than LBI-452 at the appropriate power ratio. It is expected that the CRI value of LBI-465 will be above 90. It shows that the phosphor-converted laser-based illuminant combined with optimized blue LD and red LD can render good color quality in the daily lighting fields.

IV. Conclusion

In summary, the phosphor-converted laser-based illuminant combined with blue LD and red LD was optimized concerning both color performance and BLH of lighting system. A comparative study of phosphor materials pumped by the common 452-nm LD module and the newly adopted 465-nm LD module was performed with regards to CRI, CCT, BELHER and CAF, which renders an opportunity to intentionally manipulate the spectrum distribution of LDs to obtain different characteristics of pc-LBI, owing to the large degree of freedom in spectral components. According to experiments, the highest CRI of LBI-465 is 88.7, which was 8.2% higher than that of common LBI-452. The CCT of both pc-LBIs can be tuned from 2200 K to 5000 K. High CRI and tunable CCT can satisfy different demands of lighting fields. Moreover, the BLHER of LBI-465 is 19% lower than that of LBI-452. The experimental and simulated CAF of both pc-LBIs ranges from 0.35 to 0.50. The experimental results are highly consistent with the simulation. The simulated CRI value of LBI-465 combined with red LD can be further improved to 90. Manipulated utilization of phosphor converter combined with red/blue LDs can achieve high CRI and low BLH. It proves that phosphor-converted laser-based illuminant adopted by appropriate red and blue LDs modules can realize good color quality and healthy light sources toward solid-state lighting.

Acknowledgment

The authors thank the Shandong Huaguang Optoelectronics Company, Ltd. for support of LD-based modules.

References

[1] M. R. Krames *et al.*, "Status and future of high-power light-emitting diodes for solid-state lighting," *J. Disp. Technol.,* vol. 3, no. 2, pp. 160–175, 2007.
[2] E. F. Schubert and J. K. Kim, "Solid-state light sources getting smart," *Science,* vol. 308, no. 5726, pp. 1274–1278, May 2005.
[3] S. Pimputkar *et al.*, "Prospects for LED lighting," *Nature Photon.,* vol. 3, no. 4, pp. 180–182, 2009.
[4] J. J. Wierer *et al.*, "The potential of III-nitride laser diodes for solid-state lighting," *Phys. Status Solidi C,* vol. 11, no. 3-4, pp. 674–677, 2014.
[5] R. Lachmayer *et al.*, "System efficiency of laser-based white light," *Adv. Opt. Mater.,* vol. 3, no. 5-6, pp. 523–530, 2014.
[6] M. Cantore *et al.*, "High luminous flux from single crystal phosphor-converted laser-based white lighting system," *Opt. Exp.,* vol. 24, no. 2, pp. A215–A221, Jan. 2016.
[7] K. V. Chellappan *et al.*, "Laser-based displays: A review," *Appl. Opt.,* vol. 49, no. 25, pp. F79–F98, 2010.
[8] K.-W. Tseng *et al.*, "Laser headlamp with a tunable light field," *Energies*, vol. 12, no. 4, 2019, Art. no. 707.
[9] J. Lee *et al.*, "All-fiber RGB laser light source of head-up display system for automobile application," *Curr. Opt. Photon.,* vol. 4, no. 3, pp. 221–228, 2020.
[10] N. Abu-Ageel and D. Aslam, "Laser-driven visible solid-state light source for Etendue-Limited applications," *J. Display Technol.,* vol. 10, no. 8, pp. 700–703, 2014.
[11] A. Ali *et al.*, "Blue laser diode-based remote solid-state lighting using plastic optical fiber and phosphor film for a hazardous environment," *ECS J. Solid State Sci. Technol.,* vol. 10, no. 1, 2021, Art. no. 016001.
[12] M. H. Kane *et al.*, "Laser-activated remote phosphor conversion with ceramic phosphors," in *Proc. 13th Int. Conf. Solid State Lighting*, 2014, vol. 9190, pp. 90–100.
[13] N. Trivellin *et al.*, "Laser-based lighting: Experimental analysis and perspectives," *Materials*, vol. 10, no. 10, Oct. 2017, Art. no. ma10101166.
[14] S. Li *et al.*, "Color conversion materials for high-brightness laser-driven solid-state lighting," *Laser Photon. Rev.,* vol. 12, no. 12, 2018, Art. no. 1800173.
[15] J. Wang *et al.*, "Thermally self-managing YAG:Ce–Al_2O_3 color converters enabling high-brightness laser-driven solid state lighting in a transmissive configuration," *J. Mater. Chem. C,* vol. 7, no. 13, pp. 3901–3908, 2019.
[16] Y. Ma and X. Luo, "Packaging for laser-based white lighting: Status and perspectives," *J. Electron. Packag.,* vol. 142, no. 1, 2020, Art. no. 010801.
[17] S. Liang *et al.*, "An efficient rare-earth free deep red emitting phosphor for improving the color rendering of white light-emitting diodes," *J. Mater. Chem. C,* vol. 5, no. 11, pp. 2927–2935, 2017.

[18] S. Li *et al.*, "$CaAlSiN_3:Eu^{2+}$ translucent ceramic: A promising robust and efficient red color converter for solid state laser displays and lighting," *J. Mater. Chem. C,* vol. 4, no. 35, pp. 8197–8205, 2016.

[19] Q. Zhou *et al.*, "Mn^{2+} and Mn^{4+} red phosphors: Synthesis, luminescence and applications in WLEDs. A review," *J. Mater. Chem. C,* vol. 6, no. 11, pp. 2652–2671, 2018.

[20] T. Hu *et al.*, "Glass crystallization making red phosphor for high-power warm white lighting," *Light: Sci. Appl.,* vol. 10, no. 1, pp. 1–12, Mar. 2021.

[21] Z. Liu *et al.*, "$CaAlSiN_3:Eu^{2+}$/$Lu_3Al_5O_{12}:Ce^{3+}$ phosphor-in-glass film with high luminous efficiency and CRI for laser diode lighting," *J. Mater. Chem. C,* vol. 9, no. 10, pp. 3522–3530, 2021.

[22] M. He *et al.*, "Glass-ceramic phosphors for solid state lighting: A review," *Ceram. Int.,* vol. 47, no. 3, pp. 2963–2980, 2021.

[23] Y. Zhang *et al.*, "High color rendering index composite phosphor-in-glass for high-power white laser lighting," *J. Eur. Ceram. Soc.,* vol. 41, no. 9, pp. 4915–4923, 2021.

[24] C. Wu *et al.*, "Phosphor-converted laser-diode-based white lighting module with high luminous flux and color rendering index," *Opt. Exp.,* vol. 28, no. 13, pp. 19085–19096, Jun. 2020.

[25] C. E. Reilly *et al.*, "Transmission geometry laser lighting with a compact emitter," *Phys. Status Solidi A,* vol. 217, no. 22, 2020, Art. no. 2000391.

[26] Z. Guo *et al.*, "Investigation on three-hump phosphor-coated white light-emitting diodes for healthy lighting by genetic algorithm," *IEEE Photon. J.,* vol. 11, no. 1, Feb. 2019, Art. no. 8200110.

[27] C. Xue *et al.*, "High performance non-doped blue-hazard-free hybrid white organic light-emitting diodes with stable high color rendering index and low efficiency roll-off," *Opt. Mater.*, vol. 106, 2020, Art. no. 109991.

[28] H. Chen *et al.*, "Correlated color temperature tunable white LED with a dynamic color filter," *Opt. Exp.,* vol. 24, no. 6, pp. A731–A739, Mar. 2016.

[29] X. Zhu *et al.*, "Phosphor-free, color-mixed, and efficient illuminant: Multi-chip packaged LEDs for optimizing blue light hazard and non-visual biological effects," *Opt. Laser Eng.,* vol. 134, 2020, Art. no. 106174.

[30] X. Ouyang *et al.*, "Mechanisms of blue light-induced eye hazard and protective measures: A review," *Biomed. Pharmacother.,* vol. 130, Oct. 2020, Art. no. 110577.

[31] J. X. Tao *et al.*, "Mitochondria as potential targets and initiators of the blue light hazard to the retina," *Oxidative Med. Cell Longevity,* vol. 2019, 2019, Art. no. 6435364.

[32] A. M. Colaco *et al.*, "Color characterization of multicolor multichip LED luminaire for indoor," *J. Build. Eng.*, vol. 18, pp. 19–32, Jul. 2018.

[33] J. Nie *et al.*, "Low blue light hazard for tunable white light emitting diode with high color fidelity and circadian performances," *Opt. Laser Technol.,* vol. 135, Mar. 2021, Art. no. 106709.

[34] Q. Dai *et al.*, "Circadian-effect engineering of solid-state lighting spectra for beneficial and tunable lighting," *Opt. Exp.,* vol. 24, no. 18, pp. 20049–20059, Sep. 2016.

[35] P. Zhu *et al.*, "Design of circadian white light-emitting diodes with tunable color temperature and nearly perfect color rendition," *OSA Continuum,* vol. 2, no. 8, pp. 2413–2427, 2019.

[36] J. Nie *et al.*, "Investigation on entraining and enhancing human circadian rhythm in closed environments using daylight-like LED mixed lighting," *Sci. Total Environ.,* vol. 732, Aug. 2020, Art. no. 139334.

[37] J. Fan, Y. Li, I. Fryc, C. Qian, X. Fan, and G. Zhang, "Machine-learning assisted prediction of spectral power distribution for full-spectrum white light-emitting diode," *IEEE Photon. J.,* vol. 12, no. 1, Feb. 2020, Art. no. 8200218.

[38] S.-D. Lei *et al.*, "Investigation on circadian action and color quality in laser-based illuminant for general lighting and display," *IEEE Photon. J.,* vol. 12, no. 4, Aug. 2020, Art. no. 8200509.

[39] G. Zhang *et al.*, "Spectral optimization of color temperature tunable white LEDs with red LEDs instead of phosphor for an excellent IES color fidelity index," *OSA Continuum,* vol. 2, no. 4, pp. 1056–1064, 2019.

[40] Y. Ohno *et al.*, "Color rendering and luminous efficacy of white LED spectra," in *Proc. 4th Int. Conf. on Solid State Lighting*, Bellingham, WA, USA, 2004, pp. 88–98. [Online]. Available: https://doi.org/10.1117/12.565757

[41] W. Tang *et al.*, "Blue light hazard optimization for high quality white LEDs," *IEEE Photon. J.,* vol. 10, no. 5, Oct. 2018, Art. no. 8201210.

[42] Q. Huang *et al.*, "Patterned glass ceramic design for high-brightness high-color-quality laser-driven lightings," *J. Adv. Ceram.,* vol. 11, no. 6, pp. 862–873, 2022.

[43] Y. Duan *et al.*, "Photoluminescence properties of $Tb_3Al_5O_{12}:Ce^{3+}$, Mn^{2+} phosphor ceramics for high color rendering index warm white LEDs," *Opt. Mater.,* vol. 111, 2021, Art. no. 110670.

[44] Y. Ma *et al.*, "High recorded color rendering index in single Ce,(Pr,Mn):YAG transparent ceramics for high-power white LEDs/LDs," *J. Mater. Chem. C,* vol. 8, no. 13, pp. 4329–4337, 2020.

[45] J. Nie *et al.*, "Tunable LED lighting with five channels of RGCWW for high circadian and visual performances," *IEEE Photon. J.,* vol. 11, no. 6, Dec. 2019, Art. no. 8201512.

[46] M. Wei *et al.*, "Experimental validation of colour rendition specification criteria based on ANSI/IES TM-30-18," *Lighting Res. Technol.,* vol. 52, no. 3, pp. 323–349, 2020.

[47] J. Nie *et al.*, "Optimization of the dynamic light source considering human age effect on visual and non-visual performances," *Opt Laser Technol,* vol. 145, 2022, Art. no. 107463.